International Journal of the Physical Sciences Vol. 6(16), pp. 4036-4043, 18 August, 2011
Available online at http://www.academicjournals.org/IJPS
DOI: 10.5897/IJPS10.211
ISSN 1992-1950 ©2011 Academic Journals

Full Length Research Paper

Heat transfer of intake port for hydrogen fueled port injection engine: A steady state approach

M. M. Rahman[1,2]*, Khalaf I. Hamada[1] and K. Kadirgama[1]

[1]Faculty of Mechanical Engineering, Universiti Malaysia Pahang, 26300 Pekan, Pahang, Malaysia
[2]Automotive Engineering Centre, Universiti Malaysia Pahang, 26600 Pekan, Pahang, Malaysia.

Accepted 23 May, 2011

The steady state heat transfer analysis of intake port for hydrogen fueled port injection engine is investigated. One dimensional gas dynamics was described by the flow and heat transfer in the components of the engine model. The engine model is simulated with variable engine speed and equivalence ratio (φ). Engine speed varied from 2000 to 5000 rpm with increment of 1000 rpm, while equivalence ratio changed from stoichiometric to lean limit. The effects of equivalence ratio and engine speed on heat transfer characteristics for the intake port are presented in this paper. The baseline engine model is verified with existing previous published results. Comparison between hydrogen and methane fuel was made. The obtained results show that the engine speed has the same effect on the heat transfer coefficient for hydrogen and methane fuel, while equivalence ratio has effect on heat transfer coefficient in case of hydrogen fuel only. Rate of increase in heat transfer coefficient comparison with stoichiometric case for hydrogen fuel are: 4% for (φ = 0.6) and 8% for (φ = 0.2). While negligible effect was found in case of methane fuel with change of equivalence ratio. But methane is given greater values about 11% for all engine speed values compare with hydrogen fuel under stoichiometric condition. The blockage phenomenon affected the heat transfer process dominantly in case of hydrogen fuel; however, the forced convection was influencing the heat transfer process for hydrogen and methane cases.

Key words: Heat transfer, hydrogen, methane, intake port, port injection, steady state.

INTRODUCTION

Hydrogen is a very efficient and clean fuel. Its combustion will produce no greenhouse gases, no ozone layer depleting chemicals, and little or no acid rain ingredients and pollution (Kahraman, 2005). Hydrogen, produced from renewable energy (solar, wind, biomass, tidal, etc.) sources, would result in a permanent energy system which would never have to be changed (Kahraman et al., 2007; Rahman et al., 2010). Hydrogen internal combustion engines (H_2ICE) is a technology available today and economically viable in the near-future (Rahman et al., 2009a-e). This technology demonstrated efficiencies in excess of today's gasoline engines and operate relatively cleanly (NOx is the only emission pollutant) (Boretti et al., 2007; Bakar et al., 2009). Increased efficiencies, high power density and reduced emissions are the main objectives for internal combustion engines (ICE) development (White et al., 2006). One of the major parameter that is effective in the improvement of performance and emission regulation in the ICE is the amount of heat loss from the total heat release during combustion process. So, the accurate model that describes the heat transfer phenomena for H_2ICE will give important information that is required for improving the simulation of these engines on digital computers.

The heat is converted from the intake port wall to the mixture charge. Heat transfer in this part mainly caused by forced convection, which is controlled by turbulent

*Corresponding author. E-mail: mustafizur@ump.edu.my.

Table 1. Steady state correlations constants.

Reference of previous study	*C*	*m*	*n*
Ditus and Boelter (1930)	0.023	0.800	0.4
Bauer et al. (1998) for straight manifold	0.062	0.730	0.0
Bauer et al. (1998) for curved manifold	0.140	0.660	0.0
Depcik and Assanis (2002)	0.0694	0.750	0.0
Shayler et al. (1996)	0.135	0.713	0.0

charge movement and the temperature gradient of the mixture charge to the wall. Whilst surveying the correlations for use in modeling, the quasi-steady heat transfer in the piping system of internal combustion engine, the authors noticed that these correlations mostly are based on the similarity theory developed by Nuβelt (Schubert et al., 2005).

$$\alpha = \frac{d}{k_f}.C.\mathrm{Re}^{m} \quad (1)$$

where α, d and k_f are heat transfer coefficient, cylinder diameter and fluid thermal conductivity, respectively.

Because a correlation type, easy-to-use unsteady heat transfer model is not available, classical, steady correlations in the form of $Nu = C\,Re^m$ or $Nu = C\,Re^m Pr^n$ are widely used for estimating convective heat transfer coefficient in the intake manifolds of engines (Dittus and Boelter, 1930; Shayler et al., 1996; Bauer et al., 1998; Depcik and Assanis, 2002). The constants C, m and n are adjusted to match the experimental data to account for unsteady heat transfer enhancements, surface deposits, and surface roughness. Examples of those correlations constants are listed in Table 1.

The heat transfer amount which is convected from the intake port wall to the mixture charge calculates according to the formula of Newton's law of cooling:

$$Q = \alpha A(T_g - T_w) \quad (2)$$

where Q, A, T_g and T_w are amount of heat transfer rate, heat transfer area, gas temperature and wall temperature, respectively.

Even in these correlations, the same fundamental form exists but different coefficients (C, m and n) are used and give so many different correlations. The reason there are so many different correlations is that the geometry of each engine is unique. No two engines will have the same flow patterns. Since flow is the gesture to heat transfer, the same magnitude of flow in two different engines can give two different heat transfer values. In addition, frequencies based on valve events, as well as pipe lengths, drastically alter the flow patterns and change the heat transfer relationship (Depcik and Assanis, 2002).

Besides all of these reasons, the type of the working gas which is another parameter will have a significant effect on the heat transfer process. These correlations provide reasonable agreement with experimental data in fully-developed steady pipe flows and acceptable agreement with time-resolved experimental data in unsteady flows with slow velocity variation under the quasi-steady assumption. However, for highly unsteady flows with rapid velocity variation, such as engine flows, these correlations can produce large errors in both phase and magnitude (Zeng and Assanis, 2004). Experimental results published by different researchers show that the unsteady flow effect in the engine intake manifold enhances heat transfer by 50 to 100% over the prediction of the steady pipe flow correlation presented by Dittus and Boelter (1930). At different engine speed and load conditions, the unsteadiness of the flow condition is different. Therefore, the constants (C and m) are usually optimized only for one operating condition of a given engine, and hence compromised for other conditions.

The physical properties of hydrogen fuel differ significantly from those fossil fuels (Verhelst and Sierens, 2001; Li and Karim, 2006). This provides the impetus for the authors to check up heat transfer process inside intake port for hydrogen fueled engine and specify the differences with fossil fuel (methane). So, heat transfer process will be undertaken for the present study to show the ability of the heat transfer correlations which basically found for intake port with hydrocarbons fueled engine to represent heat transfer process inside intake port with hydrogen fueled engine, as well as, features detection of heat transfer phenomenon for the intake port with the new alternative fuel.

MATERIALS AND METHODS

Engine model

A single cylinder four stroke spark ignition port injection with two

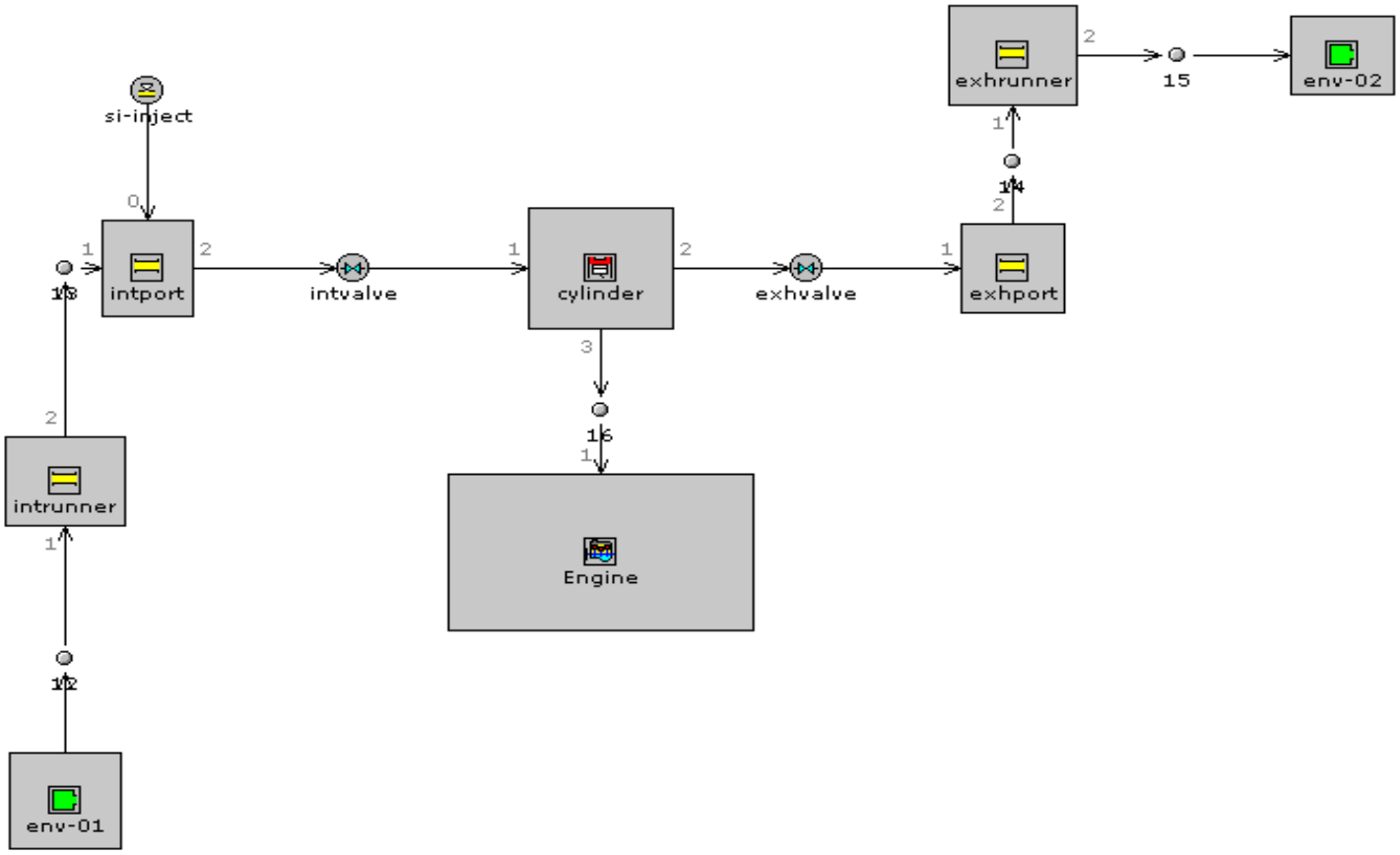

Figure 1. Model of single cylinder four stroke, port injection hydrogen fueled engine.

Table 2. Engine specifications for model A.

Parameter	Value	Unit
Bore	100	mm
Stroke	100	mm
Connecting rod length	220	mm
Compression ratio	9.5	-
Inlet valve open	9	CA(BTDC)
Exhaust valve open	55	CA(BBDC)
Inlet valve close	84	CA(ABDC)
Exhaust valve close	38	CA(ATDC)
No. of cylinder	1	-

valves (one inlet and one exhaust) model was developed utilizing GT-power software. The injection of fuel was located in the midway of the intake port. The computational model of single cylinder hydrogen fueled engine is shown in Figure 1. The engine specifications are listed in Table 1. The specific engine characteristics are used to make the model A as listed in Table 2. It is important to indicate that the intake and exhaust ports of the engine cylinder are modeled geometrically with pipes. The characteristics of the intake port of engine are listed in Table 3. The intake and exhaust ports of the engine cylinder are modeled geometrically with pipes and the air enters through a bell-mouth orifice to the pipe. The discharge coefficients of the bell-mouth orifice were set to 1 to ensure the smooth transition. The diameter and length of bell-mouth orifice pipe are 0.07 and 0.1 m, respectively and it is connected to intake air cleaner with 0.16 m of diameter and 0.25 m of length. A log style manifold was developed from a series of pipes and flow-splits. The total volume of each flow-split was 256 cm^3. The flow-splits compose from an intake and two discharges. The intake draws air from the

Table 3. Intake port characteristics.

Intake port parameter (Unit)	Value
Diameter at inlet end (mm)	40
Diameter at outlet end (mm)	40
Length (mm)	80
Surface roughness (mm)	0
Wall temperature (K)	450

preceding flow-split.

One discharge supplies air to adjacent intake runner and other supplies air to the next flow-split. The last discharge pipe was closed with a cup. The flow-splits are connected with each other through pipes with 0.09 m diameter and 0.92 m length. Intake port wall temperature value was assumed according to previous investigation results (Bauer, 1997). The junctions between the flow-splits and the intake runners were modeled with bell-mouth orifice. The intake runners were linked to the intake ports with 0.04 m diameter and 0.08 m length. The temperature of the piston is higher than the cylinder head and cylinder block wall temperature. Heat transfer multiplier is used to take into account for bends, additional surface area and turbulence caused by the valve and stem. The pressure losses are included in the discharge coefficients calculated for the valves and no additional pressure losses were used because of wall roughness (pressure losses have been estimated using dependency on Reynolds number only). The exhaust runners were modeled as rounded pipes with 0.03 m inlet diameter and 800 bending angle for runners 1 to 4 and 40° bending angle of runners 2 and 3. Runners 1 to 4 and runners 2 and 3 are connected before entering in a flow-split with 169.646 cm^3 volume. Conservation of momentum is solved in 3-dimentional flow-splits even though the flow is based on a one-dimensional version of the Navier-Stokes equation. Finally, a pipe with 0.06 m diameter and 0.15 m length connects the last flow-split to the environment. Exhaust walls temperature was calculated using a model embodied in each pipe and flow-split. The air mass flow rate in intake port was used for fuel flow rate based on the imposed equivalence ratio (φ). The specific values of input parameters including the equivalence ratio and engine speed were specified in the model. The boundary condition of the intake air was defined first in the entrance of the engine. This object describes end environment boundary conditions of pressure, temperature, and composition. The air enters through this object to the pipes. This object describes an orifice placed between any two flow components and its parts represent the plane connecting two flow components. The orifice diameter is set equal to the smaller of the adjacent component diameter on the either side of the orifice. While the orifice forward and reverse discharge coefficients are automatically calculated using the geometry of the mating flow components and orifice diameter, assuming that all transitions are sharp-edged.

The hydrogen and methane have been used to represent as a fuel in current study for revealing the difference between these fuels in term of heat transfer characteristics inside intake port.

Model governing equations

One dimensional gas dynamics model is used for representation of the flow and heat transfer in the components of the engine model. Engine performance can be studied by analyzing the mass, momentum and energy flows between individual engine components and the heat and work transfers within each component. To complete the simulation model, other additional formulas beside of the main governing equations are used for calculations of the pressure loss coefficient, heat transfer, and friction coefficient.

The heat transfer from the internal fluids to the pipe and flow split walls is dependent on the heat transfer coefficient, the predicted fluid temperature and the internal wall temperature. The heat transfer coefficient is calculated in every time step and it is a function of fluid velocity, thermo-physical properties and wall surface roughness. The heat transfer coefficient is defined as shown in Equation (3).

$$\alpha = \frac{1}{2} C_f \rho U_{eff} C_p \Pr^{-\frac{2}{3}} \quad (3)$$

where ρ, U_{eff}, C_f, C_p and Pr are the density, effective speed outside boundary layer, friction coefficient, specific heat and Prandtl number, respectively.

The friction coefficient can be expressed for smooth and rough walls as Equations (4) and (5), respectively:

$$C_f = \frac{16}{\mathrm{Re}_D} \qquad \mathrm{Re}_D < 2000 \;;\; \mathrm{Re}_D = \frac{vD}{\upsilon}$$
$$C_f = \frac{0.08}{\mathrm{Re}_D^{0.25}} \qquad \mathrm{Re}_D > 4000 \quad (4)$$

$$C_{f\,(\mathrm{rough})} = \frac{0.25}{\left(2\log_{10}\left(\frac{D}{2h}\right) + 1.74\right)^2} \quad (5)$$

where Re_D, D and h are Reynolds number, pipe diameter and roughness height, respectively.

The Prandtl number can be expresses as Equation (6).

$$\Pr = \frac{\upsilon}{\lambda} \quad (6)$$

where υ and λ are the kinematic viscosity and thermal diffusivity, respectively. The amount of heat rate which is transferred from the inlet charge inside the intake port to its wall, is calculated according to the formula of Newton's law of cooling in Equation (2).

RESULTS AND DISCUSSION

Steady state gas flow and heat transfer simulations for the in-cylinder of four stroke port injection spark ignition hydrogen fueled engine model is running for two operation parameters namely equivalence ratio (φ) and engine speed. The equivalence ratio was varied from stoichiometric limit (φ = 1.0) to a very lean limit where (φ = 0.2) with change step for the equivalence ratio equal to 0.2 and engine speed varied from 2000 to 5000 rpm with change step equal to 1000 rpm.

Model validation

The present study was approved by adopting experimental results from two previous works. General

Table 4. Specifications of the engines models.

Engine parameter	Lee et al. (1995)	Present model B	Unit
Bore × stroke	85 × 86	85 × 86	mm
TDC clearance height	NA*	3	mm
Piston pin offset	NA	1	mm
Connecting rod length	NA	150	mm
Compression ratio	8.5	8.5	-
Inlet valve open	16	16	°CA(BTDC)
Exhaust valve open	52	52	°CA(BBDC)
Inlet valve close	54	54	°CA(ABDC)
Exhaust valve close	12	12	°CA(ATDC)

*NA = not available.

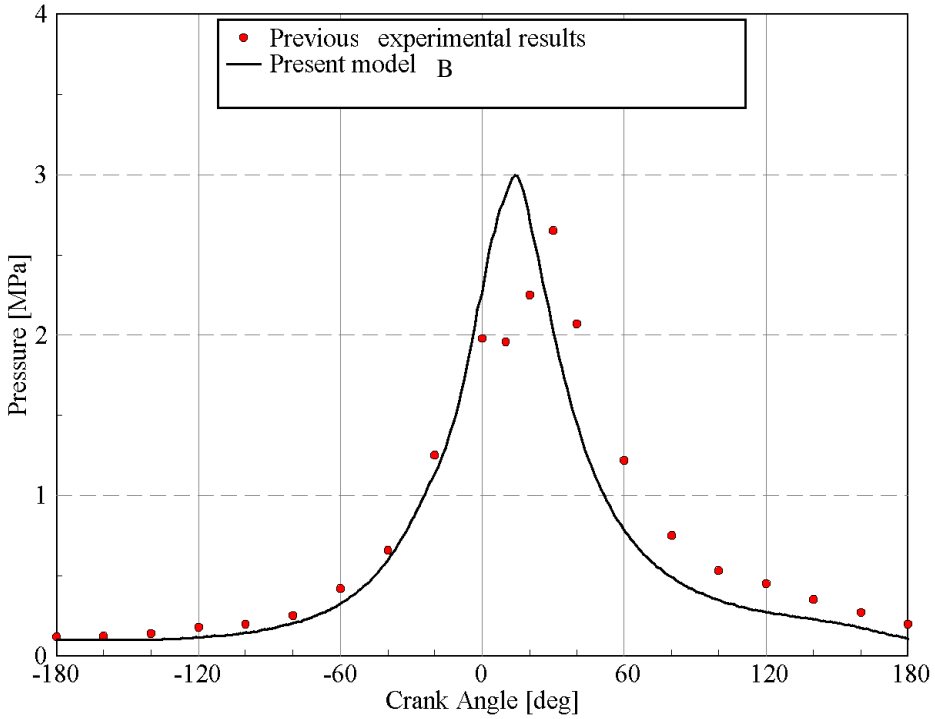

Figure 2. Comparison between published experimental results Lee et al. (1995) and present single cylinder port injection engine model B based on in-cylinder pressure.

previous existing correlation for intake port heat transfer. The experimental results obtained from Lee et al. (1995) were used for purpose of first validation in this study. Engine specifications of Lee et al. (1995) and present single cylinder port injection engine model B are listed in Table 4. The same engine model which is described in Figure 1 was used for the purpose of first validation (taking into account the difference in the engine dimensions). Engine speed and equivalence ratio were fixed at 1500 rpm and (φ = 0.5) respectively in this comparison to be coincident with Lee et al. (1995) results.

The in-cylinder pressure traces for the baseline model B and experimental previous published results Lee et al. (1995) are shown in Figure 2. It can be seen that in-cylinder pressure, trace are very good match for compression stoke and acceptable trends for expansion strokes while large deviation was obtained for

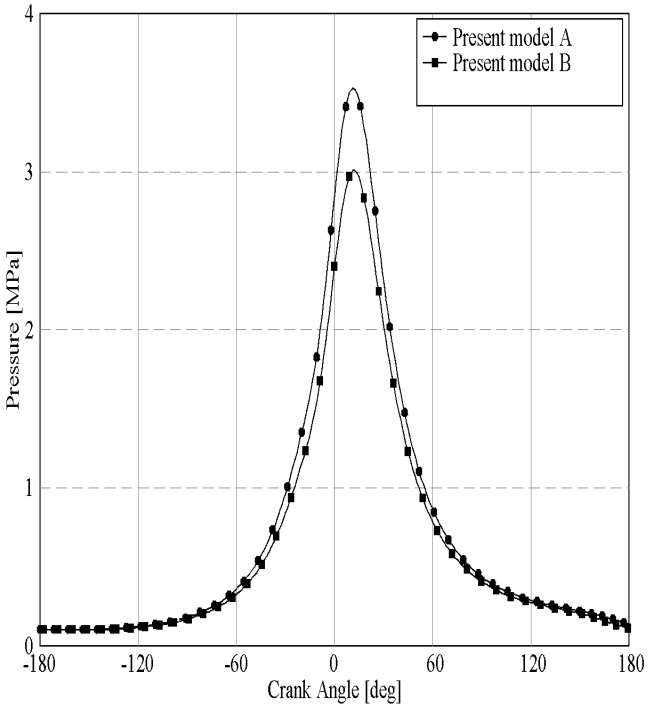

Figure 3. Comparison between models A and B based on in-cylinder pressure traces.

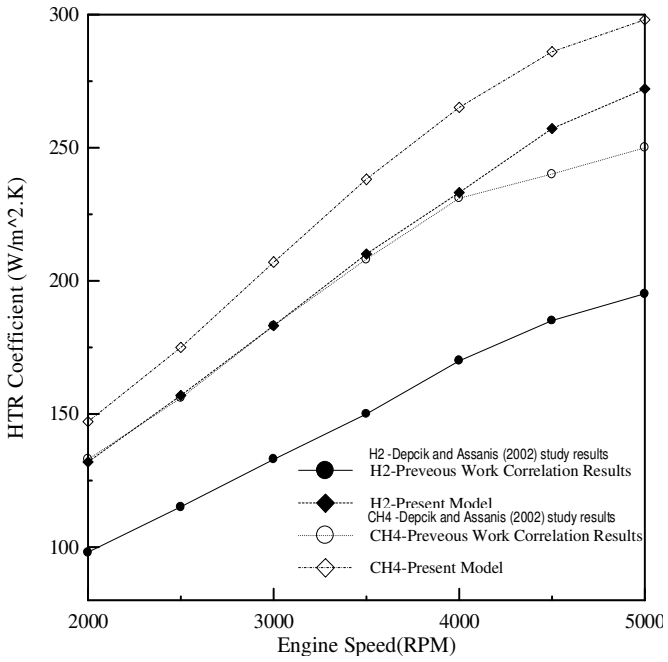

Figure 4. Comparison of heat transfer coefficient, Depcik and Assanis (2002) study results and present model A.

combustion period due to the delay in the combustion for experimental as in claim's of Lee et al. (1995) beside the difference between the some engine configuration conditions that is not mentioned in Lee et al. (1995).

However, considerable coincidence between the present model B and experimental results can be recognized in spite of the mentioned model differences. To demonstrate the effectiveness of the adopted model for the present study model A, direct comparison with model B in terms of in-cylinder pressure traces was done as shown in Figure 3. The difference between two models is due to the difference in dimensions and compression ratio between two models. Correlation which was introduced by Depcik and Assanis (2002) is used for the purpose of model verification specifically for the intake port heat transfer in present study. This correlation was proposed by using a least square curve-fit of all available experimental data to get a general relationship which describe a dimensionless heat transfer coefficient *Nu* with Reynolds number expressed as Equation (7).

$$Nu = 0.0694\,\mathrm{Re}^{0.75}\ ; \quad 1500 < \mathrm{Re} < 40000 \tag{7}$$

Direct comparison between the acquired results from the engine model A and results from empirical correlation for hydrogen and methane fuel is represented. Variation of heat transfer coefficient with engine speed for hydrogen and methane with stoichiometric mixture is revealed in Figure 4. It is clear that the correlation performance for describing methane fuel give a good agreement with engine model results, where the deviation is 11% within correlation limit and 16% outside this limit, if taking into consideration both of the deviation and limitation for the original correlation compared with the original experimental results which is used for fitting. Where correlation have an r-value (deviation factor) of 0.846, and applicable with range Reynolds number (1500<Re<40000) which correspond to engine speed values equal to (1500<RPM<4000) for methane and (1500<RPM<4500) for hydrogen (Depcik and Assanis, 2002). The same trends are achieved for the hydrogen fueled engine model. Through this comparison, the extent and reliability model adopted in the present study can be determined, while, the correlation results was under prediction for the performance of model A in case of hydrogen fuel with deviation equal to 28%. This result is expected because the correlation was derived mainly for hydrocarbon fuels.

Heat transfer coefficient for intake port

Comparison between hydrogen and methane in terms of

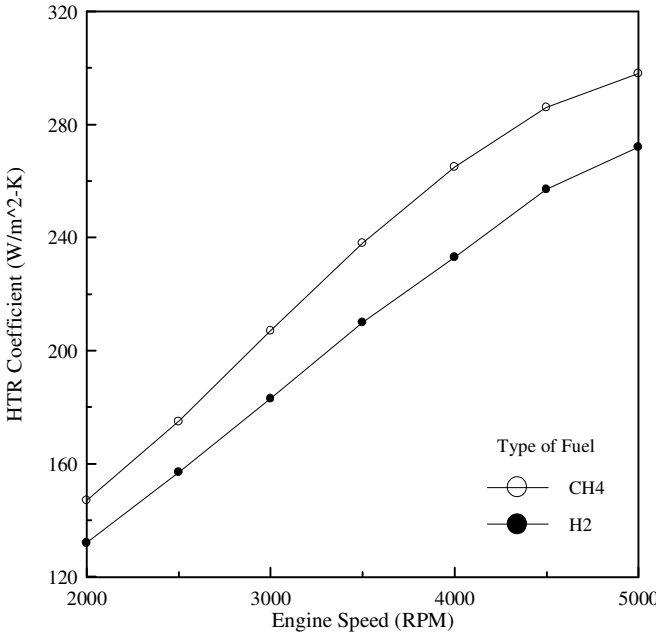

Figure 5. Variation of heat transfer coefficient with engine speed for equivalence ratio φ = 1.0.

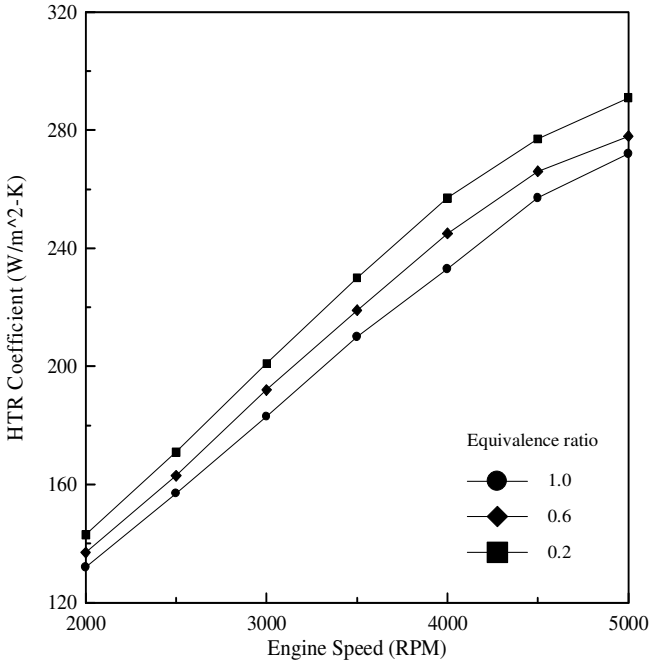

Figure 7. Variation of heat transfer coefficient for hydrogen fuel with engine speed and equivalence ratio.

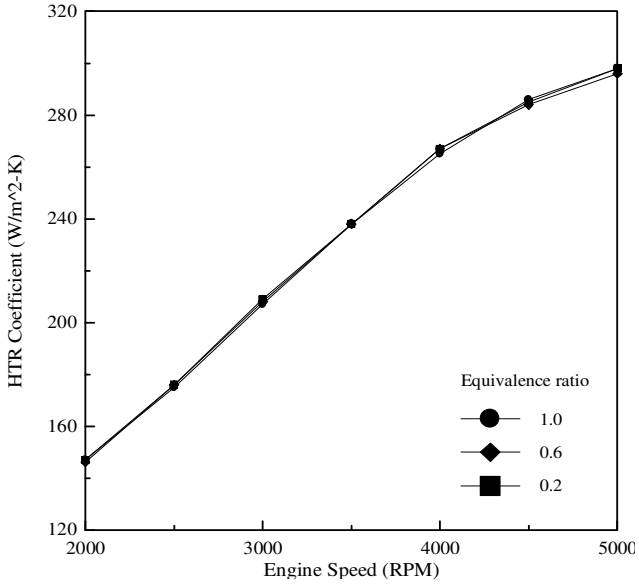

Figure 6. Variation of heat transfer coefficient for methane fuel with engine speed and equivalence ratio.

heat transfer coefficient and their behavior with changes of engine speed and equivalence ratio (φ) represent as an indicator used to reveal the characteristics of steady state heat transfer inside the intake port for port injection H_2ICE. Direct comparison between hydrogen and methane in terms of the variation of heat transfer coefficient with engine speed is described in Figure 5.

The heat transfer coefficient is increasing as engine speed increases for methane and hydrogen fuels with keeping the highest values for methane fuel. Effect of equivalence ratio (φ) on heat transfer coefficient with variation of engine speed is shown in Figures 6 and 7 for methane and hydrogen, respectively. The difference between methane and hydrogen behavior is very clear in terms of equivalence ratio (φ). In the case of methane, there are no effect (or negligible) for equivalence ratio (φ) on the values and behavior of heat transfer coefficient. As a result, it is expected that there will be no impact for this variable on the overall process of heat transfer. On the contrary, the impact of this factor in case of hydrogen is clearly seen. It decreases the equivalence ratio (φ) values heat transfer increase due to disappearance of the blockage phenomenon.

The effect of engine speed and equivalence ratio on heat transfer coefficient is clarified in case of hydrogen and methane fuels. The behavior of heat transfer coefficient is found to be governed by the blockage and forced convection effects. Forced convection effect is related to engine speed variation, while the blockage effect is related to equivalence ratio variation. In terms of engine speed, both of them (hydrogen and methane fuel) have the same trends which is increased like the heat transfer coefficient as engine speed increased due to increasing the driving force for the heat transfer process (forced convection). But methane is given greater values

about 11% for all engine speed values compare with hydrogen fuel.

Density of methane fuel is greater than hydrogen as well as the diffusion coefficient for methane is lesser than hydrogen, hence the blockage effect for hydrogen fuel is greater than methane so that the presence of forced convection with methane has more strength, due to the high restriction for the charge flow in case of hydrogen fuel; therefore, the heat transfer effect is more efficient in the case of methane fuel.

The effect of variation for the equivalence ratio (φ) in case of methane is negligible. On the other hand, the decreasing of the equivalence ratio (φ), in case of hydrogen fuel, lead to enhancement of heat transfer process due to the limitation in the blockage phenol-menon and so the gas flow become more fluently which means that the effect of the forced convection has more strength. Rate of increase in heat transfer coefficient in comparison with stoichiometric case for hydrogen fuel are: 4% for (φ = 0.6) and 8% for (φ = 0.2).

Conclusion

The present study considered the comparison in heat transfer characteristics inside the intake port for port injection engine fueled with hydrogen and methane respectively. The foregoing results indicates that heat transfer coefficient in the intake port is changed with variation of engine speed and equivalence ratio due to effect of forced convection and blockage phenomena respectively. Comparison between hydrogen and methane in terms of heat transfer coefficient and their behavior with change of engine speed and equivalence ratio are clarified that hydrogen is more dependable on equivalence ratio, whilst both of them have the same trend with engine speed variation. The blockage phenomenon was affecting the heat transfer process dominantly in case of hydrogen fuel, due to the low density and high diffusion velocity for hydrogen in comparison with methane.

ACKNOWLEDGMENT

The authors would like to acknowledge the support of Universiti Malaysia Pahang for funding under University grant no. RDU 100387 and Doctoral Scholarship Scheme (GRS 090121).

REFERENCES

Bakar RA, Mohammed MK, Rahman MM (2009). Numerical study on the performance characteristics of hydrogen fueled port injection internal combustion engine. Am. J. Eng. Appl. Sci., 2: 407-415.

Bauer WD, Wenisch J, Heywood JB (1998). Averaged and time-resolved heat transfer of steady and pulsating entry flow in intake manifold of a spark-ignition engine. Int. J. Heat and Fluid Flow. 19(1): 1-9.

Boretti AA, Brear MJ, Watson HC (2007). Experimental and Numerical Study of a Hydrogen Fuelled I.C. Engine Fitted with the Hydrogen Assisted Jet Ignition System. 16th Aust. Fluid Mechanics Conference Crown Plaza, Gold Coast, Australia. pp.1142-1147.

Depcik C, Assanis D (2002). A universal heat transfer correlation for intake and exhaust flows in an spark ignition internal combustion engine. SAE Tech. Paper No. *2002-01- 0372*.

Dittus PW, Boelter LMK (1930). Heat transfer in automobile radiators of the tubular type. Uni. California Pub. Eng., 2:443-461.

Kahraman E (2005). Analysis of a Hydrogen Fueled Internal Combustion Engine. MSc. Thesis, Graduate School of Engineering and Sciences of İzmir Instute of Technology.

performance and emission characteristics of a hydrogen fuelled spark ignition engine. Int. J. Hydro. Energy, 32(12):2066–2072.

Lee SJ, Yi HS, Kim ES (1995). Combustion characteristics of intake port injection type hydrogen fueled engine. Int. J. Hydro. Energy, 20(4):317-322.

Li H, Karim GA (2006). Hydrogen fueled spark-ignition engines predictive and experimental performance. J. Eng. Gas Turbines Power, Trans. ASME. 128(1):230-236.

Rahman MM, Hamada KI, Noor MM, Bakar RA, Kadirgama K, Maleque MA (2010). In-cylinder heat transfer characteristics of hydrogen Effects of air fuel ratio and engine speed on performance of hydrogen fueled port injection engine. J. Appl. Sci., 9:1128-1134.

Rahman MM, Mohammed MK, Bakar RA (2009b). Effect of air fuel ratio and injection timing on performance for four cylinder direct injection hydrogen engine. Eur. J. Sci. Res., 25:214-225.

Rahman MM, Mohammed MK, Bakar RA (2009c). Effects Of Engine Speed and Injection Timing And Engine Performance For 4-Cylinder DI Hydrogen Fueled Engine. Can. J. Pure Appl. Sci., 3(1):731-739.

Rahman MM, Mohammed MK, Bakar RA (2009d). Air Fuel Ratio on Engine Performance and Instantaneous Behavior of Crank Angle for Four Cylinder Direct Injection Hydrogen Fueled Engine. J. Appl. Sci. 9(16): 2877-2886.

Rahman MM, Mohammed MK, Bakar RA (2009e). Trends of Rotational Speed on Engine Performance for Four Cylinder Direct Injection Hydrogen Fueled Engine. Trends Appl. Sci. Res., 4(4):188-199.

Schubert C, Wimmer A, Chmela F (2005). Advanced heat transfer model for CI engines. SAE Tech. Paper No. *2005-01-0695*.

Shayler PJ, Colechin MJF, Scarisbrick A (1996). Heat transfer measurements in the intake port of a spark ignition engine. SAE Trans., Paper No. 960273.

Verhelst V, Sierens R (2001). Aspects concerning the optimisation of a hydrogen fueled engine. Int. J. Hydro. Energy, 26(9):981–985.

White CM, Steeper RR, Lutz AE (2006). The hydrogen-fueled internal combustion engine: a technical review. Int. J. Hydro. Energy, 31(10):1292–1305.

Zeng P, Assanis DN (2004). Unsteady convective heat transfer modeling and application to engine intake manifolds. Proc. IMECE2004 ASME, Int. Mech. Eng. Congress RD & D Expo., Paper No. IMECE2004-60068.